JET PRODUCTION IN HADRONIC PROCESSES.

Using similar arguments to those for DRELL YAN production, it is possible to study other hadronic processes.

For example, hard scattering of quarks from colliding hadrons can be studied through JET PRODUCTION.

As the final state quarks are not directly observable, the only way to determine the parton level processes is to study the final state hadrons, either singly or in jets.

(2)

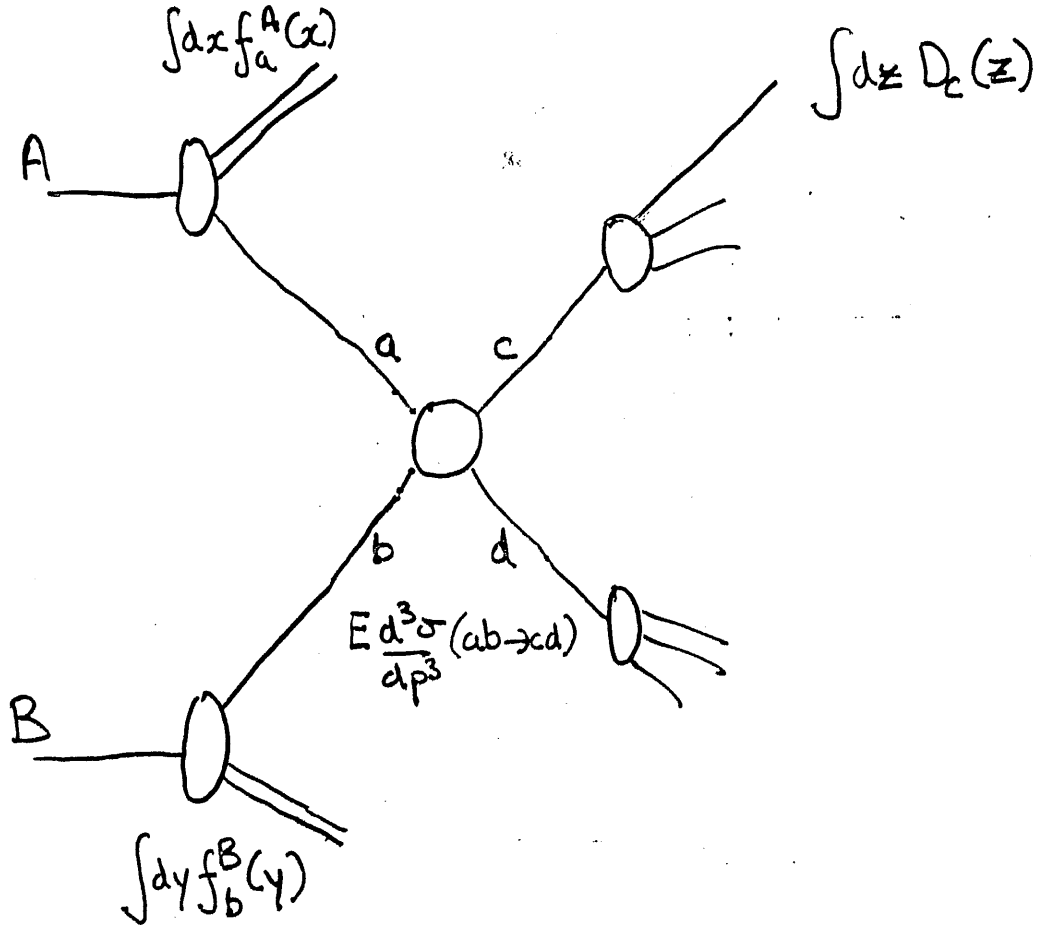

• The parton level process is described by a perturbative QCD expression for

$$E\frac{d^3\sigma}{dp^3}(ab\to cd)$$

• The initial state momentum distributions are determined by the structure functions (quark distribution functions)

• The final state hadron momentum distributions are determined by the fragmentation functions $D(z)$.

FRAGMENTATION FUNCTIONS

The assumption made is that when a quark is produced in a hard process, the probability that it will give rise to a hadron of type i with a fraction z of the initial quark momentum is independent of the process by which the quark was produced.

Within the framework of the Quark Parton Model, the number of independent fragmentation functions can be reduced to two: favoured if the produced hadron contains a quark of the same kind, unfavoured if it does not.

④ Empirically, fragmentation functions are well described by functions of the kind

$$D_i(z) \sim \frac{1}{z}(1-z)^m$$

where z is the momentum fraction carried by a hadron of type i.

The data are usually obtained from 2-jet events in e^+e^- scattering, where the problem of separating the (high p_T) quark jets from the (longitudinal) beam jets is avoided.

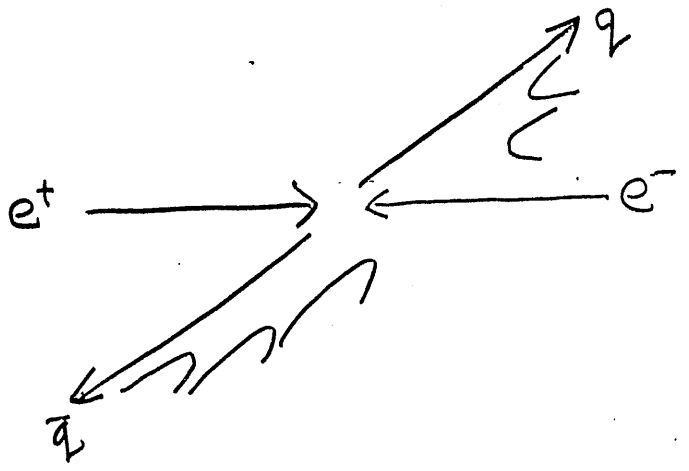

(5) PARTON LEVEL PROCESSES

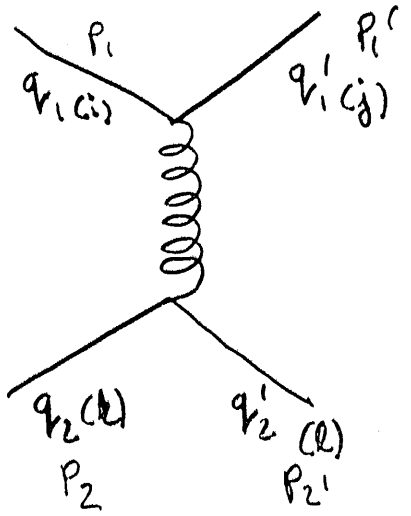

The lowest order QCD diagrams can be calculated using Feynman diagram techniques analogous to those used in QED. The calculations are in this case more complicated owing to the number of gluons.

The cross sections are of the form

$$\frac{d\sigma}{d\hat{t}}(q_1 q_2 \to q_1' q_2') = \pi \alpha_s^2(Q^2) \frac{f(\hat{\theta})}{\hat{s}^2} \delta_{q_1 q_1'} \delta_{q_2 q_2'}$$

where $\hat{s}$ is the parton level Mandelstam variable $s' = (p_1 + p_2)^2$. For high p_T scattering, $\hat{s}$ is closely related to p_T^2. Defining

$$x_T = \frac{2p_T}{\sqrt{s'}}$$

(6) it is found that the cross section can be written as

$$\frac{d\hat{\sigma}}{dp_T^2} = \frac{1}{p_T^4} f(x_T, \alpha_s(p_T^2))$$

i.e.

- At fixed x_T the partonic cross section should fall as p_T^{-4}
- The "Q^2 scale" for the process can also be fixed in terms of p_T^2.

The momentum fractions carried by the initial state quarks are of order x_T.

At sufficiently high energy (CERN collider, FNAL Tevatron), jets are relatively easy to isolate in y-ϕ space, and p_T^{-4} behaviour is seen for jet cross sections.

(7) It was argued that single particle spectra should also show p_T^{-4} behaviour.

Let the parton level differential cross section be

$$\frac{d\sigma}{dp_T} = \phi(p_T, s)$$

Assuming fragmentation is well described by a fragmentation function $D_i(z)$, the p_T distribution for a hadron produced in the fragmentation process is

$$\frac{d\sigma^{(i)}}{dp_T} = \int dp_T\, \phi(p_T)\, D_i(z)\, \delta(p_T - z p_T)\, dz$$

$$= \int \phi(p_T/z)\, D_i(z)\, \frac{dz}{z}$$

Setting

$$\phi(p_T) \sim p_T^{-n}$$

$$\frac{d\sigma^{(i)}}{dp_T} \simeq \frac{1}{p_T^n} \int D_i(z)\, z^{n-1}\, dz$$

i.e. the hadron has the same p_T dependence as the parton which generated it. This is known as the parent-child relationship.

(8) The availability of "high quality" event generators (PYTHIA, JETSET, HERWIG) allows a different strategy to be adopted. The point is that even at very high energies jets are never completely isolated owing to colour flow between the interacting partons and the spectators. This can be taken into account if identical cuts are performed on real data and a Monte Carlo sample generated with a good event generator (or, preferably, more than one, to check for systematic effects). The parton level parameters can then be adjusted so as to bring the hadron level distributions into agreement. In this way (e.g.) colour flow effects are properly taken into account, provided the event generators are good.

DIRECT PHOTONS

Our final example of a hadronic (QCD) process is direct (prompt) photon production. The principal processes have already been met in connection with DRELL YAN production.

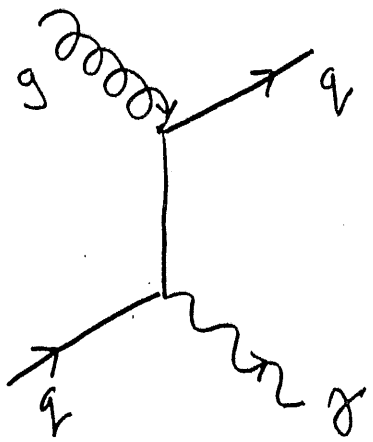

QCD Compton

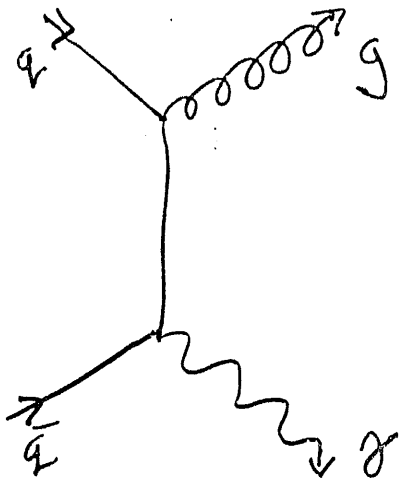

ANNIHICATION

Rearrangement of the energy-momentum balance yields a REAL photon.

$x_T = \frac{2p_T}{\sqrt{s}}$

(10) Most experiments explore the region where VALENCE quarks dominate.

This is because the Bjorken-x range for participating partons is $\sim x_T$.

For experimental reasons x_T is usually greater than 0.15, i.e. the range where valence quarks dominate.

FIXED TARGET

$2 < p_{T\gamma} < 5$ GeV/c

$p_{LAB} \sim 300$ GeV/c $\Rightarrow$ $s \sim (24)^2$ GeV^2

$.16 < x_T < .41$

UA2

$.05 < x_T < .20$ (NOT SO LARGE?!)

Empirical Evidence for Direct Photons.

- Ratio (γ/π^0) increases with p_T.
  - Most γs come from π^0 decay. If (γ/π^0) ratio increases, π^0 rejection is good in direct γ sample
  - π^0s are produced through fragmentation. At sufficiently high p_T, $z \to 1$ and $(1-z)^m$ term in $D(z)$ becomes important. Then "parent-child" relation fails and $\frac{d\sigma}{dp_T^2}(\pi^0)$ drops w.r.t. parent parton. $\frac{d\sigma}{dp_T^2}(\gamma)$ is already a parton level dependence.

- Ratio $$R = \frac{\sigma(\pi^- p \to \gamma X)}{\sigma(\pi^+ p \to \gamma X)}$$

  The ratio is expected to be greater than 1. The QCD Compton diagrams contribute to both π^+ and π^- induced production. However annihilation greatly favours π^- over π^+. (π^- is $\bar{u}d$, so 2x as many $\bar{u}u$ annihilations as $\bar{d}d$ possible; also $\frac{d\sigma}{dp_T}$ has e_i^2 factor.

A WORD OF WARNING....

The precision of direct photon predictions was greatly improved by the calculation of the full set of second order corrections (AURENCHE et al. P.L. 140B 87) However diagrams no longer separate cleanly into annihilation and QCD Compton classes.

Recent UA2 paper fits simultaneously for five distribution functions.

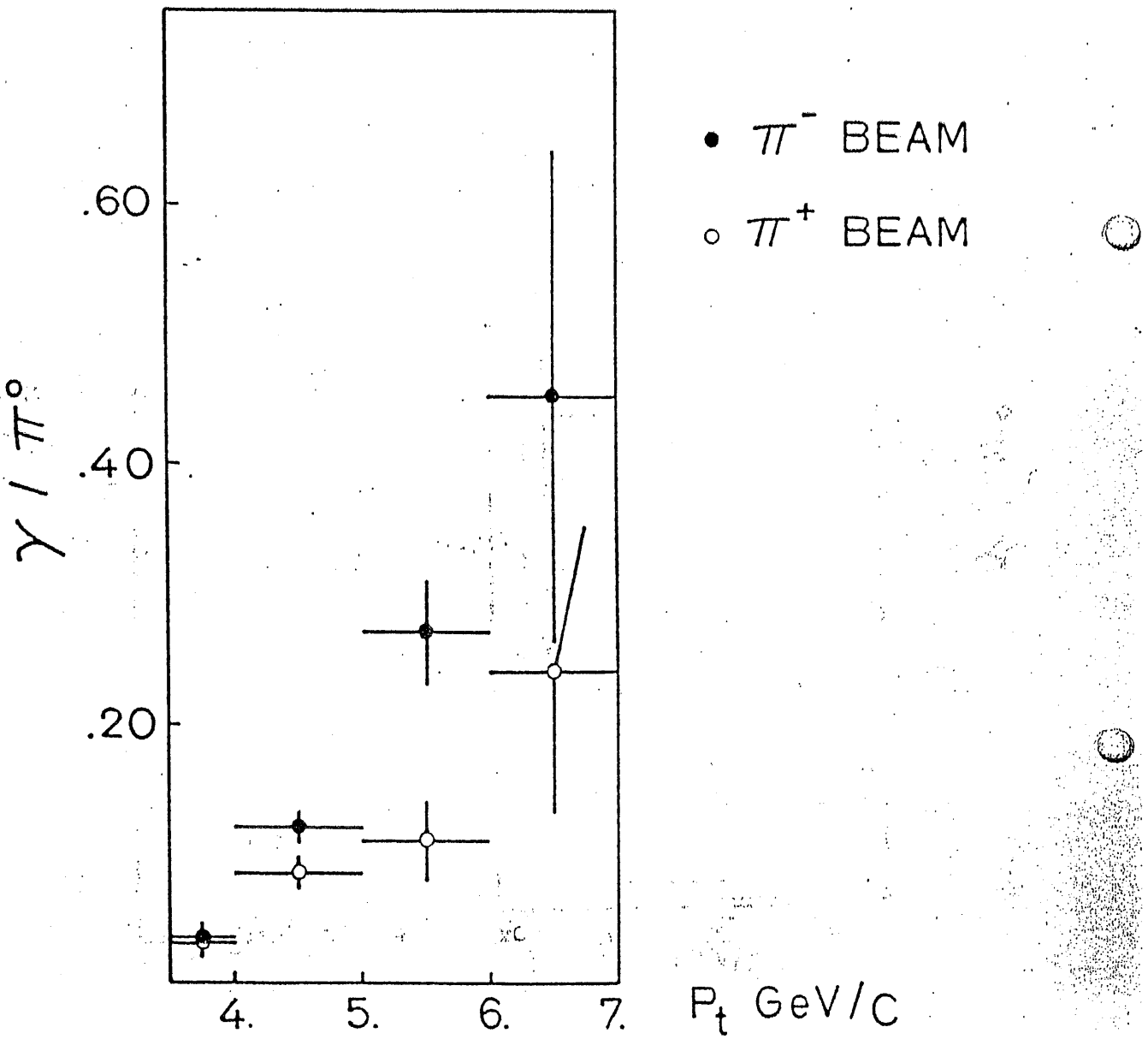
WA70 DATA
280 GeV/c $\pi^{\pm}$ p
• π^- BEAM
○ π^+ BEAM
γ / π^0
.60
.40
.20
4.
5.
6.
7.
P_t GeV/C

FIG. 5

NUCLEAR EFFECTS
THE EMC EFFECT

The development of structure functions assumes that measurements are done on NUCLEON targets, or at worst very light isoscalar targets.

BUT

This means using a *liquid Hydrogen* target (or Deuterium). Liquid Hydrogen is not very dense ($\rho = 0.0708\ g\ cm^{-3}$), leading to LOW EVENT RATES (or very extended targets).

SO

For *practical* reasons, nuclear targets, which can be much denser, are preferable.

At the relatively high Q^2 values typical of Deep Inelastic Scattering, it was assumed that scattering off a nuclear target could be described as an incoherent superposition of scattering off nucleon targets.

$$F_2^A(x) = \frac{1}{A}\left[Z\,F_2^p(x) + (A-Z)\,F_2^n(x)\right]$$

for a nuclear target of charge Z and mass A.

This was expected to break down near $x=0$ (SHADOWING) and near $x=1$ (FERMI MOTION).

In between, it was supposed that the superposition picture would be valid. [It is in any case used as the definition of $F_2^A(x)$.]

(3)

ORIGINAL EMC DATA

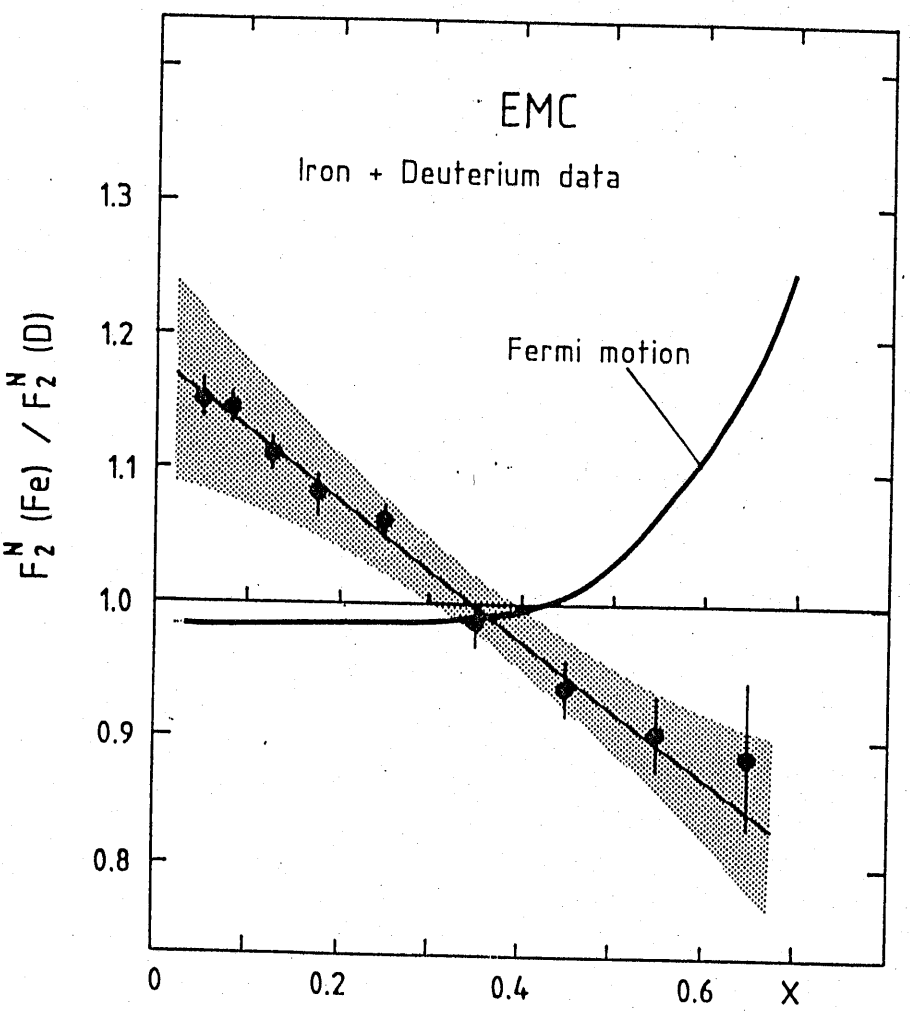

Small correction
for neutron excess in Fe
to make it into isoscalar target.

Apparently, ratio drops LINEARLY from $x = 0.1$ to $x = 0.6$

FIG. 2.4

Looked like a single effect

(4)

EMC (1992)

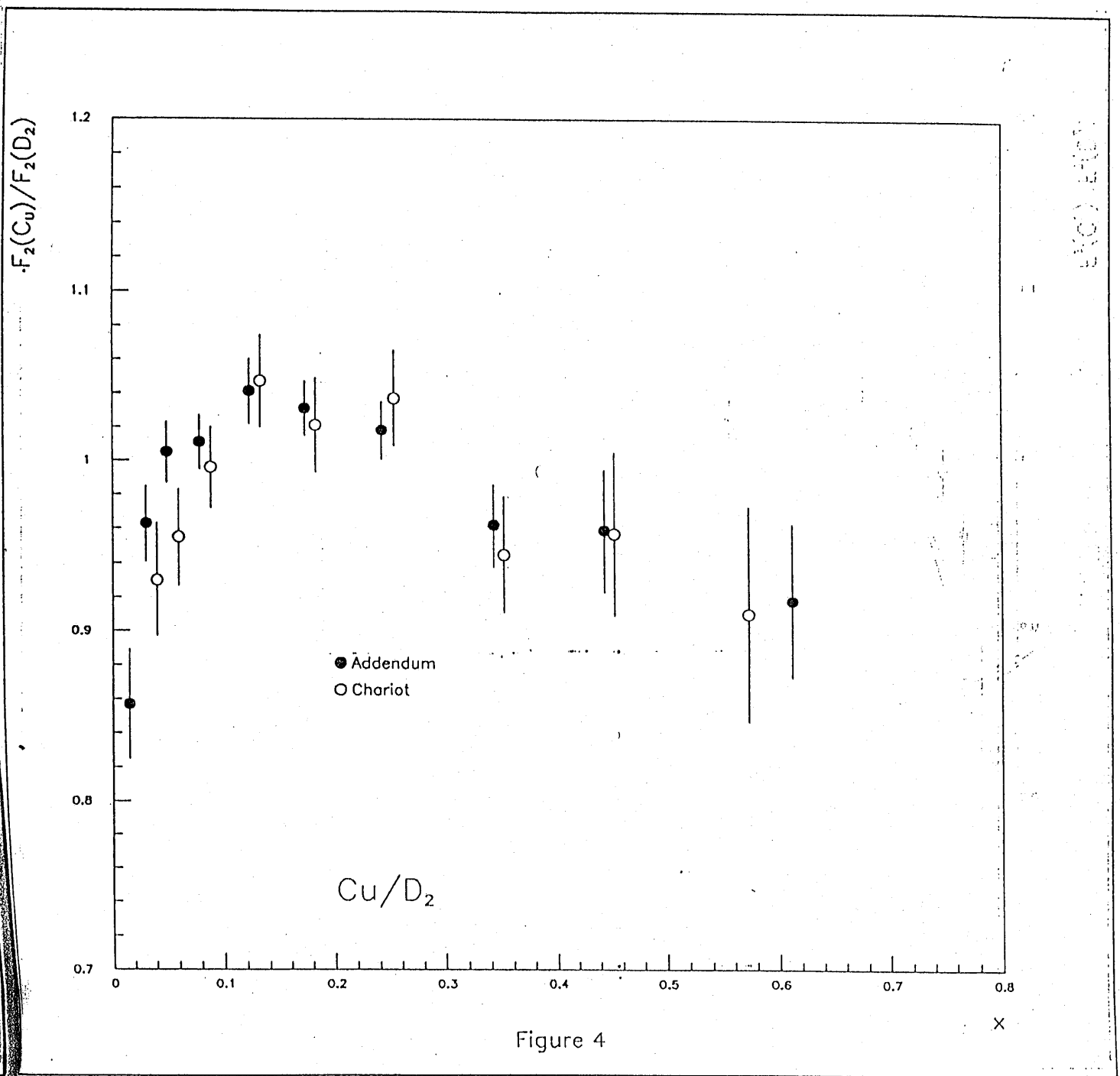

Figure 4

NMC

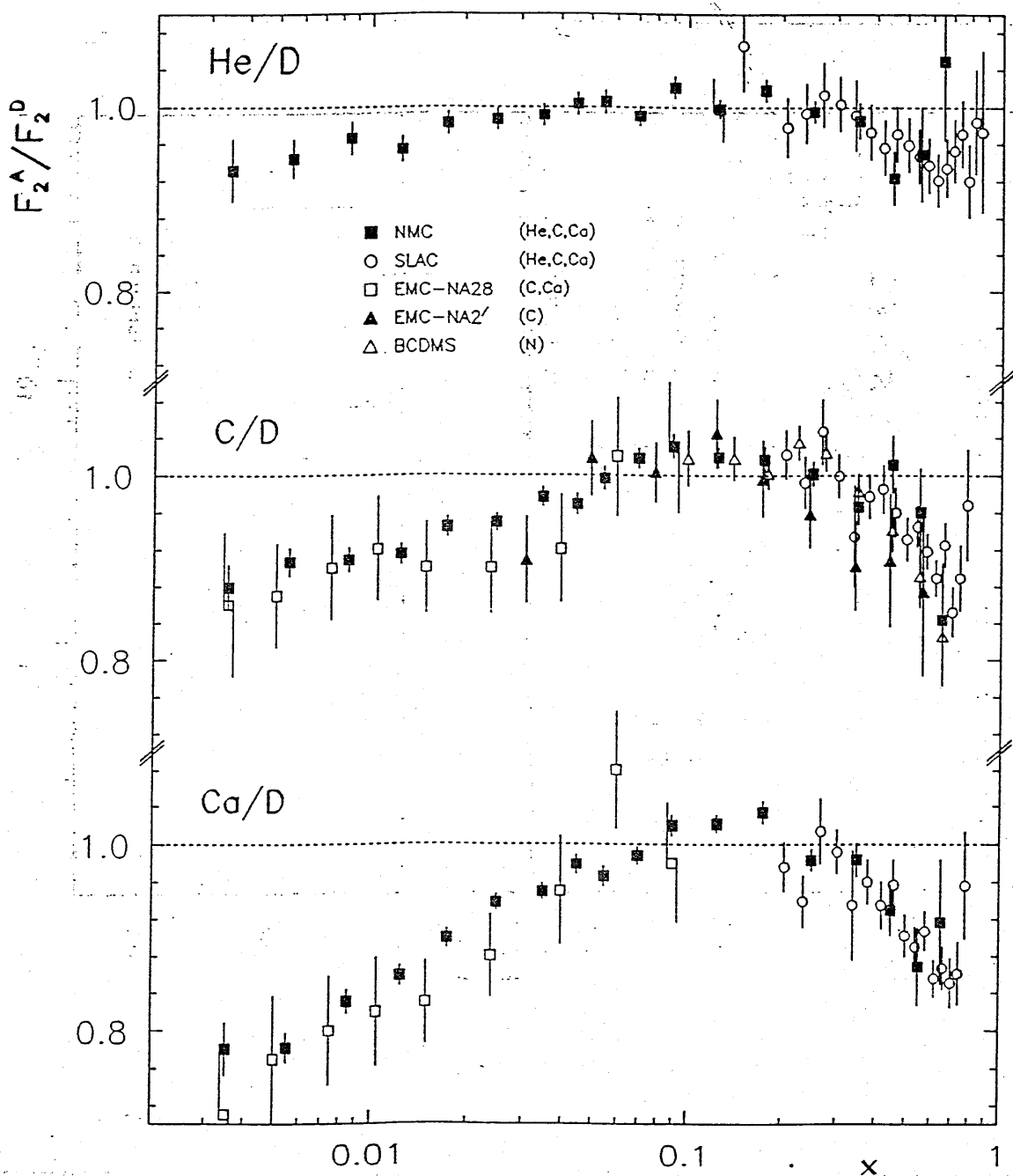
He/D
C/D
Ca/D
F_2^A/F_2^D
1.0
0.8
NMC (He,C,Ca)
SLAC (He,C,Ca)
EMC–NA28 (C,Ca)
EMC–NA2′ (C)
BCDMS (N)
0.01
0.1
1
x

FIG. 2.14

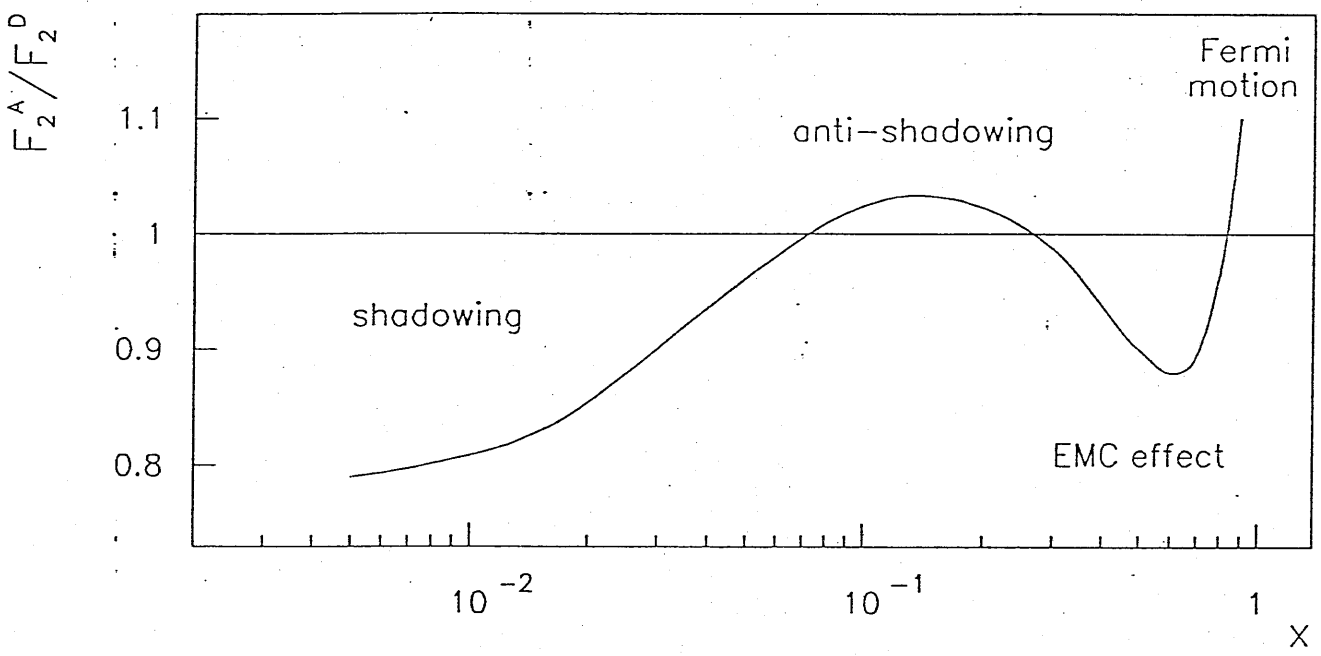
F_2^A/F_2^D
1.1
1
0.9
0.8
shadowing
anti−shadowing
Fermi
motion
EMC effect
10^{-2}
10^{-1}
1
X

FIG. 1.3

These data have been studied intensively, both because they are interesting in themselves and in order to validate the conclusions built up over many years using data from nuclear targets.

Dozens of models have been put forward to account for this behaviour. We shall look at

SHADOWING — VECTOR DOMINANCE MODEL

PARTON FUSION MODEL

EMC — NUCLEAR BINDING MODEL

Q^2 RESCALING MODEL

FERMI MOTION

SHADOWING

VECTOR DOMINANCE MODEL

Consider a photon of 4-momentum $q_\mu = (\nu, \underline{k})$. It can fluctuate into a vector meson of mass M_V. The energy of the fluctuation is

$$E_V = \sqrt{M_V^2 + k^2}$$

with $Q^2 = -q^2$, $k^2 = \nu^2 + Q^2$, i.e the "original" energy of the photon is

$$\nu = \sqrt{-Q^2 + k^2}$$

So the energy uncertainty is

$$\Delta E = E_V - \nu \underset{\nu \text{ large}}{\approx} \frac{Q^2 + M_V^2}{2\nu}$$

Then the coherence length, i.e. the length over which the fluctuation takes place, is

$$d(M_V^2, Q^2) = \Delta t \approx \frac{1}{\Delta E} \approx \frac{2\nu}{Q^2 + M_V^2} = \frac{1}{Mx} \cdot \frac{1}{(1 + M_V^2/Q^2)}$$

(9) The mean free path for the vector meson is

$$\ell(M_V^2) = \frac{1}{\sigma_V(M_V^2)\, n_0}$$

n_0 – nucleon density

$\sigma_V(M_V^2)$ – c.s. for interactions of vector mesons of mass M_V with a nucleon.

The necessary conditions for shadowing are then

$$d(M_V^2, Q^2) > \ell(M_V^2)$$
$$R_A > \ell(M_V^2)$$

Note that the expression for the coherence length implies

- that shadowing becomes more important as $x \to 0$,
- that shadowing becomes less important as $Q^2 \to \infty$.

The (strong interaction) cross sections for the vector meson components are considerably larger than the (electromagnetic) bare photon cross section.

This means the photon flux is depleted as it passes through the nucleus, leading to a lower effective number of nucleons "seen" than would be expected from superposition.

This accounts for the drop in F_2^A/F_2^D as $x \to 0$.

PARTON FUSION (RECOMBINATION)

From uncertainty arguments, the longitudinal distance in which a parton with momentum fraction x can be localized is

$$\Delta z \sim \frac{1}{x P_N}$$

while the Lorentz-contracted mean separation between nucleons in a nucleus (seen in the BREIT frame) is

$$\Delta z_N \sim 2 R_N \frac{M}{P_N}$$

i.e. for some x ($x < x_N = 1/(2R_N M)$) partons at a fixed impact parameter start to overlap in space. Under these conditions, these 'soft' partons can recombine. Momentum conservation leads to

- a depletion at low x (SHADOWING)
- a replenishment at somewhat higher x (ANTI SHADOWING)

(12) Note that this explanation would suggest that the distribution functions themselves change, while in VMD the effect stems from the properties of the probe.

(2.27)

NUCLEAR BINDING

Conventional models of nuclear binding suggest other hadrons (π, Δ, ...) are included in the nucleus. If so, scattering could take place off them. For π exchange only, where z is the fraction of the nuclear momentum carried by the nucleon/pion, we have

$$F_2^A(x) = \int_x^A f_N(z)\, F_2^N(x/z)\, dz + \int_x^A f_\pi(z)\, F_2^\pi(x/z)\, dz$$

$F^\pi(x)$ is the pion structure function.

More generally, for n_{spe} species of hadron

$$F_2^A(x) = \sum_i^{n_{spe}} \int_x^1 dz\, f_i(z)\, F_2^i(x/z)$$

In general, with enough hadron species, this model will always fit the data, but so loses its predictive power. Reasonable results are obtained with π, N and Δ.

Q^2 RESCALING

Here, the idea is that in nuclear matter the effective size of the nucleon increases (no explanation*) so a γ of given energy probes with a shorter effective de Broglie wavelength

$$\lambda' = \lambda (R_N/R_A)$$

As λ' is related to Q^2, we should set

$$F_2^A(x, Q^2) = F_2^N(x, \xi_A Q^2) \quad (\xi_A > 1)$$

where

$$\xi_A \simeq R_A^2/R_N^2$$

More precisely, if Q^2-evolution is taken into account, one finds

$$\xi_A(Q^2) = \left(R_A^2/R_N^2\right)^{\alpha_s(Q_0^2)/\alpha_s(Q^2)}$$

The observed behaviour of $F_2^{Fe}(x)/F_2^D(x)$ is obtained for $\xi \sim 1.15$

* [illegible] "[illegible]" [illegible]

(15) FERMI MOTION

As $x \to 1$, the ratio $F^A(x)/F^p(x)$ in the end inevitably rises sharply.

While for a fixed target one normally uses

$$x = Q^2/2M_\nu$$

it would be more correct to use the Lorentz-covariant form

$$x = Q^2/2P.q$$

since P takes into account the (Fermi) motion of the nucleon inside the nucleus. Thus we write

$$F_2^A(x) = \int_x^A f_N(z)\, F_2^N(x/z)\, dz$$

where $f_N(z)$ is the momentum distribution of nucleons inside the nucleus, and

$$z = A(q.p)/(q.P_A)$$

i.e. A times the fraction of the nucleus momentum carried by the struck nucleon. As z is generally >1, this samples $F_2^N(x')$ for lower values of x' than x, the convoluted value. As $x \to 1$, this leads to

$$F_2^A(x) \gg F_2^N(x)$$

RATIO OF CROSS SECTIONS FROM ν DATA

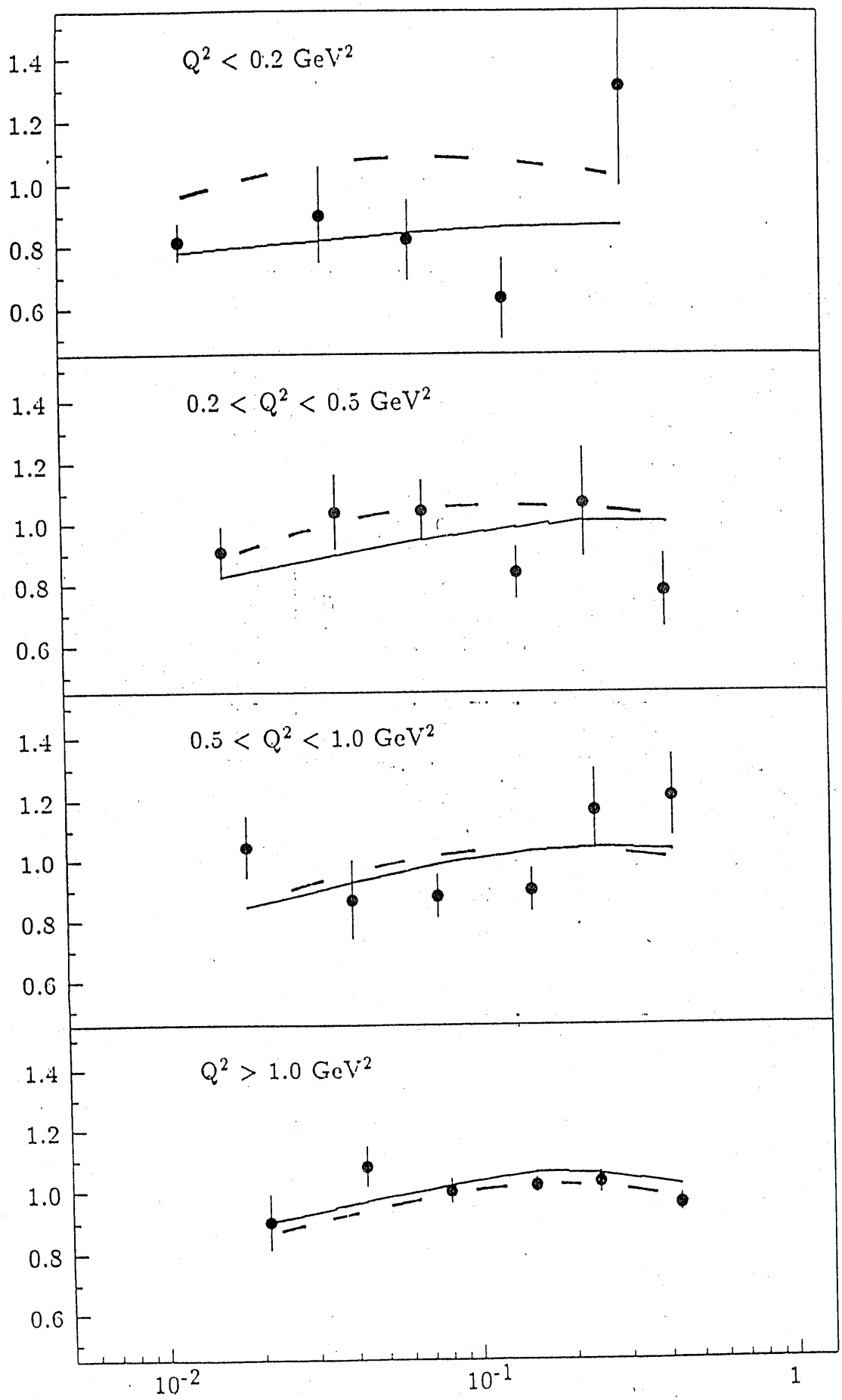

WA59
BEBC

FIG. 2.27

SPIN STRUCTURE FUNCTION OF THE PROTON

Most measurements of deep inelastic scattering involve UNPOLARIZED targets. This condition is built into the "summing and averaging" of initial and final state helicities used to prepare amplitudes for trace theorem techniques.

However, relativistic lepton beams are naturally polarized. Information on how spin is shared among partons can be obtained by measuring scattering with a POLARIZED target.

METHOD. [N.P. B328 (1989) 1]

Using targets polarized longitudinally parallel and antiparallel to the beam, it is possible to measure the resulting cross sections $d\sigma^{\uparrow\uparrow}$ and $d\sigma^{\uparrow\downarrow}$ and the asymmetry

$$A = \frac{d\sigma^{\uparrow\downarrow} - d\sigma^{\uparrow\uparrow}}{d\sigma^{\uparrow\downarrow} + d\sigma^{\uparrow\uparrow}}$$

This (experimental) asymmetry is related to the virtual photon-nucleon asymmetries A_1 and A_2 by

$$A = D(A_1 + \eta A_2)$$

where D and η are functions of the kinematic variables.

$$A_1 = \frac{\sigma_{1/2} - \sigma_{3/2}}{\sigma_{1/2} + \sigma_{3/2}}$$

$$A_2 = \sigma_{TL}/\sigma_T$$

$\sigma_T = \frac{1}{2}(\sigma_{1/2} + \sigma_{3/2})$ transverse photoabsorption σ

σ_{TL} longitudinal-transverse interference

STRUCTURE FUNCTIONS

$$\frac{d^2\sigma^{\uparrow\downarrow}}{dQ^2 d\nu} - \frac{d^2\sigma^{\uparrow\uparrow}}{dQ^2 d\nu} = \frac{4\pi\alpha^2}{E^2 Q^2}\left[M(E+E'\cos\theta)G_1(Q^2,\nu) - Q^2 G_2(Q^2,\nu)\right]$$

In the scaling region (Q^2, ν large), we define new structure functions $g_1(x), g_2(x)$ such that

$$M^2\nu\, G_1(Q^2,\nu) \longrightarrow g_1(x)$$

$$M^2\nu\, G_2(Q^2,\nu) \longrightarrow g_2(x)$$

These can be correlated with the asymmetries A_1, A_2 as follows

$$A_1 = (g_1 - \gamma^2 g_2)\frac{1}{F_1}$$

$$A_2 = \gamma(g_1 + g_2)\frac{1}{F_1}$$

where $\gamma = \sqrt{\frac{2Mx}{E\nu}}$

Hence

$$g_1 = F_1(A_1 + \gamma A_2)$$

Now, since γ, η are both small, $A_1 = A/D$ and

$$g_1^{(p)} \triangleq F_1\frac{A}{D} = \frac{A}{D}\frac{F_2}{2x(1+R)}$$

INTERPRETATION OF $g_1^{(p)}(x)$

The asymmetry A_1 can be interpreted in the QPM.

Let $q_i^{+(-)}(x)$ be the distribution function for quarks of species i, having charge e_i and helicity parallel (antiparallel) to the nucleon.

Then

$$A_1 = \frac{\sigma_{1/2} - \sigma_{3/2}}{\sigma_{1/2} + \sigma_{3/2}} = \frac{\sum_i e_i^2 (q_i^+(x) - q_i^-(x))}{\sum_i e_i^2 (q_i^+(x) + q_i^-(x))}$$

as

$$F_1(x) = \tfrac{1}{2} \sum_i e_i^2 (q_i^+(x) + q_i^-(x))$$

and $g_1(x) = A_1 F_1$, it follows that

$$g_1(x) = \tfrac{1}{2} \sum_i e_i^2 (q_i^+(x) - q_i^-(x)) \equiv \tfrac{1}{2} \sum_i e_i^2 \Delta q_i$$

SUM RULES

There are two sum rules frequently quoted in connection with spin structure functions. Using current algebra, BJORKEN obtained

$$\int_0^1 [g_1^p(x) - g_1^n(x)]dx = \frac{1}{6}\frac{g_A}{g_V}\left(1 - \frac{\alpha_s}{\pi}\right)$$

[BJORKEN SUM RULE]

This sum rule is regarded as a rigorous QCD requirement.

Making a number of additional assumptions (Su(3) flavour symmetry, no polarization of strange quark sea) Ellis and Jaffe obtained a sum rule for $g_1^{(p)}(x)$

$$\int_0^1 g_1^p(x)dx = \frac{1}{12}\frac{g_A}{g_V}\left[1 + \frac{5}{3}\cdot\frac{(3F/D - 1)}{(F/D + 1)}\right] = 0.189 \pm .005$$

for EMC kinematic region.

(6) EMC made simultaneous measurements on two oppositely polarized Ammonia targets in a polarized beam. The polarizations were swapped regularly to reduce systematics.

The resultant measurement was

$$\int_0^1 g_1^p(x)\,dx = 0.126 \pm 0.010 \pm 0.015$$

This is INCOMPATIBLE (3σ level) with the ELLIS-JAFFE sum rule.

(7) INTERPRETATION

$$I_p = \int_0^1 g_1^p(x)dx = \frac{1}{2}\left[\frac{4}{9}\tilde{\Delta}u + \frac{1}{9}\tilde{\Delta}d + \frac{1}{9}\tilde{\Delta}s\right]$$

$$I_n = \int_0^1 g_1^n(x)dx = \frac{1}{2}\left[\frac{1}{9}\tilde{\Delta}u + \frac{4}{9}\tilde{\Delta}d + \frac{1}{9}\tilde{\Delta}s\right]$$

where

$$\tilde{\Delta}q = \int_0^1 (q^+ - q^- + \bar{q}^+ - \bar{q}^-)dx$$

The EMC measurement gives

$$I_p = 0.126 \pm 0.018$$

The BJORKEN sum rule gives

$$I_p - I_n = 0.209$$

so (neglecting $\tilde{\Delta}s$)

$$0.126 \pm 0.018 = \tfrac{1}{2}\left(\tfrac{4}{9}\tilde{\Delta}u + \tfrac{1}{9}\tilde{\Delta}d\right)$$

$$-0.083 \pm 0.018 = \tfrac{1}{2}\left(\tfrac{1}{9}\tilde{\Delta}u + \tfrac{4}{9}\tilde{\Delta}d\right)$$

Solving

$$\tilde{\Delta}u = 0.7 \pm 0.07 \leftarrow$$

$$\tilde{\Delta}d = -0.55 \pm 0.07 \leftarrow$$

errors anticorrelated

In this simple model the fraction of the proton spin carried by the quarks is

$$\tilde{\Delta}u + \tilde{\Delta}d = 0.15 \pm 0.13$$

Extra input is required to include the strange quarks. This is usually done using data from WEAK HYPERON DECAYS and invoking $SU(3)_{FLAVOUR}$ symmetry. This gives

$$(\tilde{\Delta}u + \tilde{\Delta}d - 2\tilde{\Delta}s)/\sqrt{3} = 0.397$$

One then obtains

$$\langle S_z \rangle_u = \tfrac{1}{2}\tilde{\Delta}u = 0.391 \pm 0.016 \pm 0.023$$

$$\langle S_z \rangle_d = \tfrac{1}{2}\tilde{\Delta}d = -0.236 \pm 0.016 \pm 0.023$$

$$\langle S_z \rangle_s = \tfrac{1}{2}\tilde{\Delta}s = -0.095 \pm 0.016 \pm 0.023$$

so

$$\langle S_z \rangle_{quarks} = +0.06 \pm 0.047 \pm 0.069$$

Note that the requirement from conservation of angular momentum is

$$\frac{1}{2}\sum_i \Delta q_i + \Delta G + \langle L_z \rangle = \frac{1}{2}$$

where

$$\Delta G = \int_0^1 dx \, (G_\uparrow(x) - G_\downarrow(x))$$

is the net helicity carried by GLUONS.

The result is SURPRISING. At present no reconciliation of this result with the success of the static quark model in predicting (e.g.) magnetic moments has been achieved.

Experimentally SMC will combine hydrogen [BUTANOL) with Deuterium measurements so as to obtain $g_1^n(x)$ directly and so test the BJORKEN sum rule.